Original Article

Thalamic functional connectivity on 7-Tesla magnetic resonance imaging and its relation to motor signs in early-stage Parkinson's disease

Xiaoyu Wang[1,2], Yongqin Xiong[2], Jianxing Hu[2], Fengzhu Li[3], Caohui Duan[2], Haoxuan Lu[2], Dong Zhang[2], Jiayu Huang[2], Xiangbing Bian[2], Song Wang[2], Miao Wang[3], Xi Yin[3], Zhongbao Gao[3], Xin Lou[1,2]

[1]School of Medicine, Nankai University, Tianjin, China; [2]Department of Radiology, Chinese PLA General Hospital, Beijing, China; [3]Department of Neurology, the Second Medical Center & National Clinical Research Center for Geriatric Disease, Chinese PLA General Hospital, Beijing, China

Contributions: (I) Conception and design: X Wang; (II) Administrative support: X Lou, Z Gao; (III) Provision of study materials or patients: All authors; (IV) Collection and assembly of data: All authors; (V) Data analysis and interpretation: All authors; (VI) Manuscript writing: All authors; (VII) Final approval of manuscript: All authors.

Correspondence to: Xin Lou, MD, PhD. School of Medicine, Nankai University, 94 Weijin Road, Tianjin 300071, China; Department of Radiology, Chinese PLA General Hospital, 28 Fuxing Road, Beijing 100853, China. Email: louxin@301hospital.com.cn; Zhongbao Gao, MD. Department of Neurology, the Second Medical Center & National Clinical Research Center for Geriatric Disease, Chinese PLA General Hospital, 28 Fuxing Road, Beijing 100853, China. Email: gaozb301@163.com.

Background: It is well known that dysfunction of thalamocortical circuity generates the motor signs that lead to distinct disease processes and prognoses in Parkinson's disease (PD). This study aimed to leverage ultrahigh-field magnetic resonance imaging (MRI) to identify the connectivity alterations of thalamocortical circuity and clarify their relation to motor signs in early PD.

Methods: Patients with early-stage PD (n=55) and healthy controls (HCs, n=56) were recruited from March 2022 to July 2023. All participants underwent 7-Tesla MRI scans as the baseline. Sign scores were calculated from the Movement Disorder Society Unified Parkinson's Disease Rating Scale III. Significant differences in the functional connectivity between the thalamus subregions and cortex between the PD and HC groups were discovered. The association between altered thalamic functional connectivity and sign scores was evaluated using Spearman or Pearson correlation analysis with false discovery rate (FDR) correction.

Results: Compared to the HCs, the patients with early-stage PD exhibited a decreased functional connectivity between thalamic subregions (primary motor, sensory, occipital, premotor, and parietal thalamus regions) and the cortex [voxel-level P<0.001, cluster-level $P_{\text{family-wise error (FWE)}}$ <0.05]. Further exploration of the connection pattern within thalamic subregions showed that the connection strength between the primary motor and sensory (t=2.055; P=0.042), sensory and occipital (t=2.173; P=0.032), and occipital and parietal (t=2.365; P=0.020) regions were reduced. Importantly, motor signs in early-stage PD were associated with the alterations of functional connectivity pattern between the parietal thalamus and left dorsolateral part of the superior frontal gyrus (r=–0.272; P_{FDR} =0.049) and the right thalamus (r=–0.267; P_{FDR} =0.048) .

Conclusions: These findings support the use of ultrahigh-field MRI for examining the thalamic subregions and clarifying their involvement in the neural mechanisms of various motor signs in early-stage PD.

Keywords: Parkinson's disease (PD); ultrahigh field; magnetic resonance imaging (MRI); thalamus; motor sign

Submitted Jul 22, 2024. Accepted for publication Nov 14, 2024. Published online Dec 18, 2024.
doi: 10.21037/qims-24-1498
View this article at: https://dx.doi.org/10.21037/qims-24-1498

Introduction

Parkinson's disease (PD) is a progressive neurodegenerative disease characterized by resting tremor, bradykinesia, rigidity, and postural balance disorder (1). Generally, the expression and predominance of each classic clinical sign vary from patient to patient. Studies have shown that different motor features in PD can be used to monitor therapeutic responses and to assess the processes and prognoses of diseases (2,3). Moreover, the neuropathological hallmark of PD is the depletion of nigrostriatal dopaminergic system; however, it primarily reflects the terminal stages of the disease but not the motor and non-motor impairments in early-stage PD (4). Therefore, exploring quantitative imaging markers for different motor signs of early-stage PD is crucial.

The thalamus, considered an important hub in thalamocortical circuity, is a comprehensive relay node for transmitting diverse information (5). Many studies have examined the thalamus to investigate how basal ganglia-thalamocortical circuits are affected in PD in order to generate deeper insights into the underlying mechanism and pathophysiology of the disease (6-8). Bu *et al.* found that differences in the functional connectivity density of the bilateral premotor thalamus could differentiate between the PD subtypes of tremor dominant (TD) and postural instability and gait difficulty (PIGD) (6). A prospective longitudinal study reported that alterations in bilateral thalamus morphology could predict conversion to freezing of gait in patients with PD (8). Over the years, the thalamus has also become a target area for surgical treatments in PD (9). Deep brain stimulation (DBS) and magnetic resonance imaging (MRI)-guided focused ultrasound (MRgFUS) targeting the thalamus can effectively improve motor signs in patients with PD (10,11). These recent studies have confirmed the role of the thalamus in modulating the cortical activity associated with motor signs, disease progression, and surgical efficacy in PD.

Clinical MRI studies, including those using a conventional clinical field of 1.5 and 3 Tesla (T), have reported several measures of changes in the functional connectivity between various substructures of the thalamus and various cortical regions in PD (12-15). However, these conventional clinical fields currently lack the sensitivity and specificity of scope required to fully characterize elements of thalamic subregions (16). Therefore, their related connections and changes have not been examined with sufficient thoroughness to contextualize the changes associated with PD. Ultrahigh-field MRI scanners, especially the 7-T types, when combined with bold-oxygenation-level-dependent (BOLD) functional MRI (fMRI), provides a powerful tool for investigating the alterations in functional connectivity in small thalamic subregions (17,18). This research approach has gradually gained recognition in its ability to reveal the pathogenesis of nervous system diseases, such as schizophrenia, trigeminal neuralgia, and major depressive disorder (16,17,19).

We hypothesized that alterations in thalamic functional connectivity as detected by ultrahigh-field BOLD fMRI between patients with PD and healthy controls (HCs) could provide new evidence for understanding the different motor signs of PD. To test our hypothesis, in this study, we (I) applied a voxel-based analysis to the functional neuroimaging data to identify a differential connectivity pattern between the thalamic subregion and cortex, (II) analyzed the thalamic subregion characteristics based on a region of interest (ROI)-wise approach to further clarify this connectivity pattern, and (III) applied Pearson or Spearman correlation analysis to characterize its signatures for motor signs. We present this article in accordance with the STROBE reporting checklist (available at https://qims.amegroups.com/article/view/10.21037/qims-24-1498/rc).

Methods

Ethical considerations

The study was conducted in accordance with the Declaration of Helsinki (as revised in 2013) and was approved by the Chinese PLA General Hospital Ethics Committee (No. S2022-572-01). Informed consent was obtained from all individual participants. The ethical approval included construction of a comprehensive assessment system for neurodegenerative diseases based on multimodal imaging. The same ethical approval number applies to in multiple related studies due to the broad scope of the approval.

Participants

The protocol of this study was registered in the ClinicalTrials.gov database (NCT06449404). A total of 145 patients with PD were initially recruited for this study from March 2022 to July 2023. Two neurologists assessed each patient's clinical state and diagnosed PD according to the Movement Disorder Society (MDS) Clinical Diagnostic Criteria (20). Early-stage PD is defined as Hoehn and Yahr

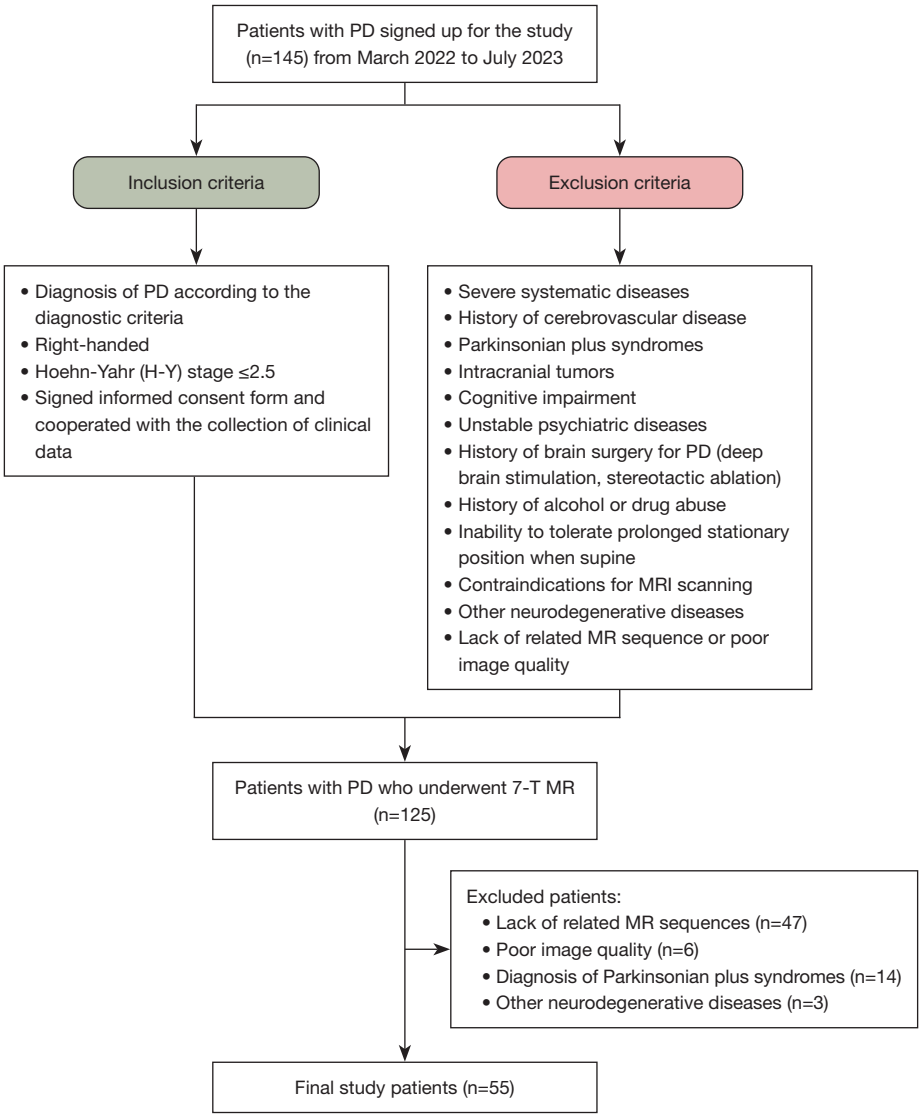

Figure 1 Flowchart of study participants with early-stage PD. PD, Parkinson's disease; MRI, magnetic resonance imaging; MR, magnetic resonance.

Scale (H-Y) score between 1 and 2.5 (3). The inclusion and exclusion criteria for early-stage PD are shown in *Figure 1*. Finally, we included 55 patients with right-handed PD, and 56 age- and gender-matched right-handed HCs were recruited from the community for analysis.

Clinical assessment

Basic demographic data including age, gender, and years of education were collected. Among patients with PD, the data also included years of disease duration and the levodopa equivalent daily dose (LEDD). The MDS Unified Parkinson's Disease Rating Scale (MDS-UPDRS) was used to evaluate the disease severity of PD, which consists of part I (nonmotor daily living experience), part II (motor daily living experience), part III (motor examinations), and part IV (motor complications). We also calculated the sign scores of MDS-UPDRS III items that represented four major motor signs in early-stage PD (21): bradykinesia, rigidity, tremor, and axial signs. Additionally, gait scores were further calculated in a subanalysis. The method employed for calculating motor signs is available in the

Supplementary file (Appendix 1). The Mini-Mental State Examination (MMSE) was applied to evaluate cognitive function. The normal MMSE scores in this study were used the cutoff points as follows (22): illiterate, >17; literate to a grade school level, >20; and literate to a level of junior high school or higher education, >23.

MRI acquisition

The experiment was performed on a whole-body 7-T scanner (MAGNETOM Terra, Siemens Healthineers, Erlangen, Germany) equipped with an 8-channel transmit and 32-channel receive coil. A resting-state fMRI (rsfMRI) scan was performed with echo-planar imaging (EPI) as follows: voxel =1.8×1.8×1.8 mm^3, repetition time (TR) =2,000 msec, echo time (TE) =24 msec, flip angle =90°, field of view (FOV) =216 mm × 216 mm, matrix =120×120, slice thickness =1.8 mm, and interleaved slices =80. Each functional run produced 240 volumes.

MRI data preprocessing

Data Processing and Analysis for Brain Imaging (DPABI) software (http://www.rfmri.org/dpabi) was used to preprocess the rsfMRI data, including motion correction, removal of the top 10 time points, slice timing, normalization to Montreal Neurological Institute (MNI) space, nuisance regression, detrending, smoothing with a 4-mm full width at half maximum (FWHM), and band-pass filtering (0.008–0.08 Hz).

Calculation of functional connectivity

Functional connectivity was defined as the correlation of time series between brain regions as measured by the Pearson correlation coefficient and reflected the temporal coherence between brain regions. DPABI software was used to build functional connectivity. The ROI was defined as the brain regions outlined in the Oxford thalamic connectivity atlas (23). This atlas is generated using diffusion-based structural connectivity in white matter between the thalamus and cortex, which segments the thalamus into seven subregions, with >25% probability of connection to seven exclusive cortical areas, respectively. Therefore, many voxels within a subregion can still have anatomical connections to other brain regions (23), which also applies to functional connectivity. Seed-based analysis was carried out using each thalamic subregion as a seed, and a whole brain connectivity map (z values) to each seed was calculated. ROI-wise analyses were calculated on seven regions to obtain the connection strength within the thalamic subregions.

Statistical analysis

Statistical analyses and plots were performed using SPSS 26 (http://www.spss.com/) software (IBM Corp., Armonk, NY, USA) and GraphPad Prism version 9 (https://www.graphpad.com/) software (GraphPad Software, Boston, MA, USA), respectively. The Shapiro-Wilk test was used to check normality of the data distribution. The two-sample independent *t*-test was used to analyze the continuous variables (e.g., age, years of education), while the χ^2 test was used to analyze the dichotomous variables (e.g., sex).

Statistical Parametric Mapping software (SPM12; Wellcome Centre for Human Neuroimaging, London, UK) was used for statistical analysis of the MRI data. A whole-brain voxel-wise-dependent *t*-test was used to identify significant alterations in functional connectivity between the early-stage PD and HC group [voxel $P<0.001$ and cluster $P<0.05$, with family-wise error (FWE) correction]. Age, sex, and education were entered as covariates. Significant clusters of thalamic connectivity were reported based on the Automated Anatomical Labeling (AAL) atlas (24) to identify anatomical regions. Subsequently, the significant values of brain regions were extracted. Spearman or Pearson correlation analysis was used to evaluate the relationship between thalamic functional connectivity and clinical scores. The results of correlation analysis were corrected by the false discovery rate (FDR) to ensure accuracy. The significance threshold was set at a two-tailed P value <0.05.

Results

Demographic information and clinical characteristics

The group of 55 patients with early-stage PD who underwent 7-T MRI scan had a mean age of 61.98±1.02 years and a mean disease duration of 4.50±0.39 years. Among the patients, 27 patients were female, and 28 patients were male. The mean value of the H-Y score was 1.75±0.94 which was an appropriate stage for early-stage PD. Other demographic and clinical characteristics of early-stage patients with PD and HCs are shown in *Table 1*. There were no significant differences between the two groups (*Table 1*) in terms of age, sex, or years of education (all

Table 1 Demographic and clinical characteristics of the included participants with early-stage PD and the HC groups

Variable	Early PD (n=55)	HC (n=56)	t/χ^2 value	P value
Age (years)	61.98±1.02	64.48±0.79	−1.950	0.054
Sex (male/female)	28/27	21/35	2.023	0.155
Education (years)	11.46±0.67	12.73±0.42	−1.627	0.107
Disease duration (years)	4.50±0.39	–	–	–
MMSE	26.20±0.53	–	–	–
H-Y stage	1.75±0.94	–	–	–
LEDD (mg/day)	475.45±29.78	–	–	–
MDS-UPDRS				
I	7.84±0.60	–	–	–
II	9.15±0.72	–	–	–
III	25.78±1.44	–	–	–
IV	0.84±0.23	–	–	–
Total	43.60±2.34	–	–	–
Sign scores		–	–	–
Tremor	3.82±3.50	–	–	–
Axial signs				
Axial[1]	6.09±3.87	–	–	–
Axial[2]	4.80±3.14	–	–	–
Gait	1.29±0.98	–	–	–
Rigidity	6.29±3.29	–	–	–
Bradykinesia	9.56±5.73	–	–	–

Data are presented as the mean ± standard deviation or number. PD, Parkinson's disease; HC, healthy control; MMSE, Mini-Mental State Examination; H-Y stage, Hoehn and Yahr stage; LEDD, levodopa-equivalent daily dose; MDS-UPDRS, Movement Disorder Society Unified-Parkinson Disease Rating Scale; Axial[1], with gait score; Axial[2], without gait score.

P values >0.05).

Brain functional connectivity alterations between thalamic subregions and the cortex in the early-stage PD and HC groups

We compared the early-stage PD and HC groups in terms of the alteration in functional connectivity between the thalamic subregions and cortex. Five subregions of the thalamus showed significant differences in the functional connectivity between two groups, including the primary motor thalamus, sensory thalamus, occipital thalamus, premotor thalamus, and posterior parietal thalamus (*Table 2* and *Figure 2*). The other subregions showed no significant difference between the two groups.

With primary motor thalamus as the seed region, there was a reduction in functional connectivity to the cortex, including the left rectus, bilateral temporal pole, bilateral lingual gyrus (LING), left thalamus, left rolandic operculum, bilateral superior temporal gyrus (STG), and right middle occipital gyrus (voxel-level P<0.001, cluster-level P_{FWE} <0.05).

With the sensory thalamus as the seed region, there was a decreased functional connectivity between the cortex and right temporal pole (TPOsup.R), left rectus, left LING, left rolandic operculum, left medial orbital part of the superior frontal gyrus (ORBsupmed.L), left thalamus, left opercular part of the inferior frontal gyrus (IFGoperc.L),

Table 2 Voxel-based analysis of thalamic functional connectivity in the early-stage PD and HC groups (HC group > PD group)

Cluster ID	Brain region	Hemisphere	Cluster size (voxels)	Peak MNI coordinate (mm)			Peak-level *t* value	Voxel-level P	Cluster-level P_{FWE}
				x	y	z			
Subregion 1 (connection to primary motor region)								<0.001	<0.05*
1	REC	L	133	−10	26	−14	5.067		
2	TPOsup	R	556	60	10	−8	5.518		
3	LING	L	386	−14	−52	2	5.561		
4	TPOsup	L	69	-50	12	−14	4.839		
5	LING	R	107	20	−72	0	4.559		
6	THA	L	80	−16	−18	0	4.233		
7	ROL	L	127	−46	−12	16	4.519		
8	STG	L	84	−56	−40	22	4.594		
9	STG	R	26	42	−34	16	4.387		
10	MOG	R	78	48	−68	26	4.551		
Subregion 2 (connection to sensory region)								–	–
1	TPOsup	R	300	54	10	−14	5.992		
2	REC	L	74	−12	28	−18	4.403		
3	LING	L	595	−14	−54	0	5.561		
4	ROL	L	284	−44	−16	16	4.920		
5	ORBsupmed	L	76	−4	66	−2	4.890		
6	THA	L	93	−22	−28	6	5.036		
7	IFGoperc	L	101	−38	14	20	4.895		
8	MTG	L	7	−44	−42	10	4.982		
9	DCG	R	110	8	22	32	4.358		
10	DCG	L	52	−12	−36	50	4.177		
11	SMA	R	119	6	10	56	4.547		
Subregion 3 (connection to occipital region)								–	–
1	STG	R	1181	64	−18	−4	5.779		
2	TPOsup	L	14	−18	10	−32	5.217		
3	PHG	R	111	28	−16	−24	5.269		
4	STG	L	852	−52	−14	10	5.727		
5	SFGmed	L	52	−2	70	8	4.328		
6	SPG	R	17	10	−82	48	5.324		
7	DCG	L	130	−12	−36	46	4.790		
8	SPG	R	100	16	−56	70	4.599		
9	PCUN	L	62	−12	−58	66	4.250		

Table 2 (*continued*)

Table 2 (*continued*)

Cluster ID	Brain region	Hemisphere	Cluster size (voxels)	Peak MNI coordinate (mm)			Peak-level *t* value	Voxel-level P	Cluster-level P_{FWE}
				x	y	z			
Subregion 5 (connection to premotor region)								–	–
1	ORBsupmed	L	29	–8	66	–4	4.135		
2	LING	L	39	–14	–52	2	4.026		
3	ROL	L	70	–48	–10	14	4.282		
Subregion 6 (connection to posterior region)								–	–
1	STG	R	1054	60	–32	18	5.412		
2	HIP	R	59	28	–16	–22	4.761		
3	STG	L	949	–58	–2	–10	5.240		
4	SFGdor	L	109	–18	62	28	4.705		
5	THA	R	47	12	–16	–2	5.259		
6	IFGtriang	R	80	54	32	14	4.548		
7	DCG	R	27	2	16	30	3.985		
8	DCG	L	111	–14	–36	46	4.658		
9	SMA	L	20	–10	–4	48	4.349		
10	DCG	R	75	14	–34	46	4.735		
11	PreCG	L	80	–38	–26	58	3.893		

*, the voxel-level threshold was P<0.001, with cluster-level P_{FWE} <0.05. The brain regions are reported based on the Automated Anatomical Labeling atlas: DCG, median cingulate and paracingulate gyri; HIP, hippocampus; IFGoperc, inferior frontal gyrus, opercular part; IFGtriang, inferior frontal gyrus, triangular part; LING, lingual gyrus; MOG, middle occipital gyrus; MTG, middle temporal gyrus; ORBsupmed, superior frontal gyrus, medial orbital; PCUN, precuneus; PHG, parahippocampal gyrus; PreCG, precentral gyrus; REC, gyrus rectus; ROL, rolandic operculum; SFGdor, superior frontal gyrus, dorsolateral; SFGmed, superior frontal gyrus, medial; SMA, supplementary motor area; SPG, superior parietal gyrus; STG, superior temporal gyrus; THA, thalamus; TPOsup, temporal pole: superior temporal gyrus. PD, Parkinson's disease; HC, healthy control; MNI, Montreal Neurological Institute; FWE, family-wise error.

left middle temporal gyrus, bilateral median cingulate and paracingulate gyri (DCG), and right supplementary motor area (SMA) (voxel-level P<0.001, cluster-level P_{FWE} <0.05).

With the occipital thalamus as the seed region, there was a decrease in functional connectivity between the cortex and bilateral STG, left temporal pole (TPOsup.L), right parahippocampal gyrus, left medial part of superior frontal gyrus, right superior parietal gyrus, left DCG, and left precuneus (voxel-level P<0.001, cluster-level P_{FWE} <0.05).

There was also decreased functional connectivity between the premotor thalamus and the ORBsupmed, LING, and rolandic operculum in the left hemisphere.

With the posterior parietal thalamus as the seed region, there was decreased functional connectivity between the cortex and the bilateral STG, right hippocampus, left dorsolateral part of the superior frontal gyrus (SFGdor.L), right thalamus, right triangular part of the inferior frontal gyrus, bilateral DCG, left SMA, and left precentral gyrus (voxel-level P<0.001, cluster-level P_{FWE} <0.05).

Brain functional connectivity alterations within thalamic subregions in the early-stage PD and HC groups

To observe the alterations of the functional connectivity within thalamic subregions, we further conducted ROI-wise analysis (*Figure 3*). There were significant differences between the PD and HC groups in terms of functional connectivity between the primary motor and sensory thalamus (t=2.055; P=0.042), sensory and occipital thalamus (t=2.173; P=0.032), and occipital and parietal thalamus (t=2.365, P=0.020) (*Figure 3*). There were no significant differences in the functional connectivity between the

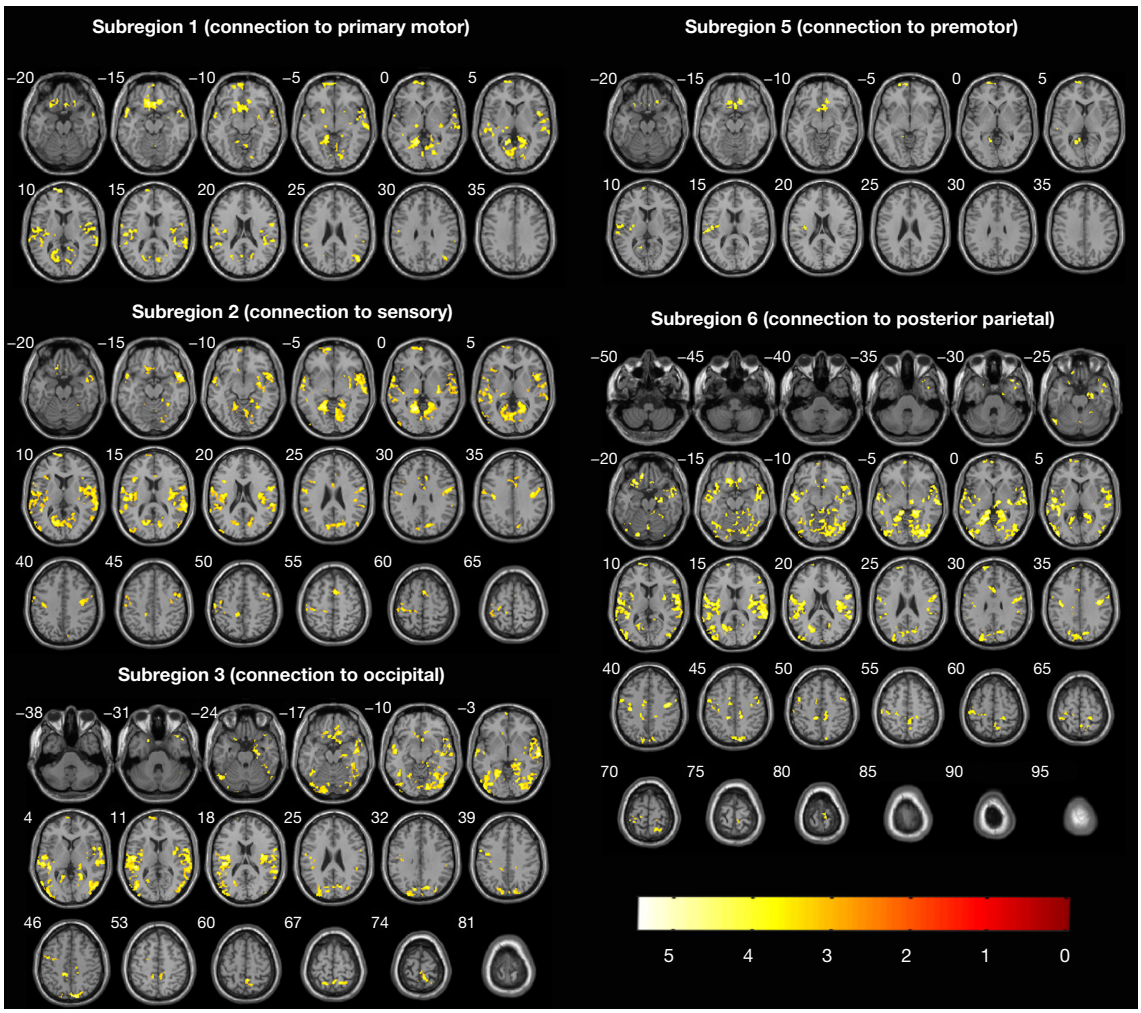

Figure 2 Voxel-based analysis for thalamic functional connectivity in the early-stage PD and HC groups. Five subregions of the thalamus showed significant differences in the functional connectivity, with decreased activity in patients with early-stage PD compared to HCs. The color bar represents the t value. PD, Parkinson's disease; HC, healthy control.

target regions including the prefrontal thalamus, premotor thalamus, and temporal thalamus and the other six thalamic subregions, respectively (P>0.05). These results of ROI-wise analysis are shown in Table S1.

Correlations between brain functional changes and clinical scores

Spearman or Pearson correlation analysis was conducted to investigate the relationship between functional connectivity in the related brain regions and clinical scores (*Figure 4*). The results revealed that the connectivity between the parietal thalamus and right thalamus and between the parietal thalamus and SFGdor.L were negatively correlated with rigidity (r=–0.272; P_{FDR} =0.049) score and gait score (r=–0.267; P_{FDR} =0.048), respectively. Other results of correlation analysis did not pass FDR correction and are shown in Table S2.

Discussion

This is the first study to use ultrahigh-field MRI to investigate the alterations in thalamic functional connectivity associated with different motor signs in early-stage PD. We identified a decreased connectivity pattern between the thalamic subregion and other brain regions in patients with PD as compared to HCs. Additionally, this decreased connectivity pattern was also confirmed among

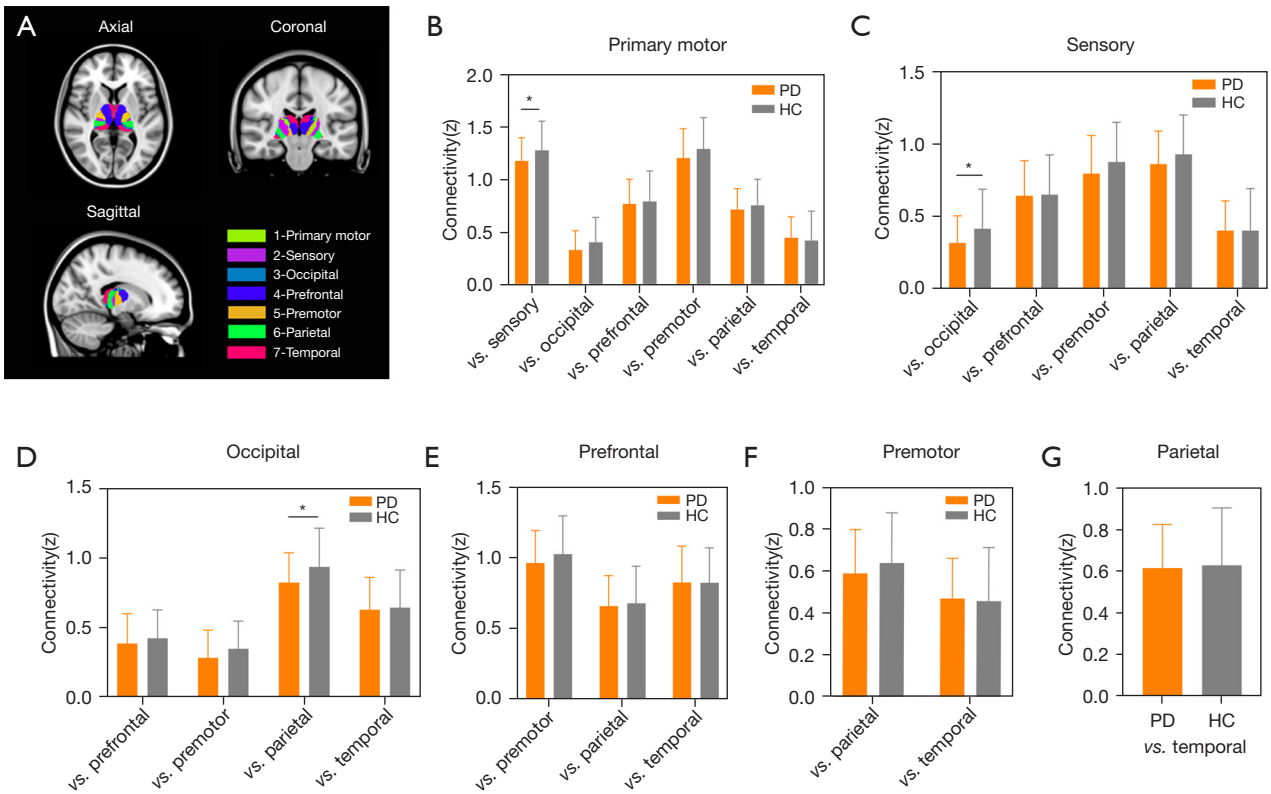

Figure 3 ROI-based analysis of thalamic functional connectivity in the early-stage PD and HC groups. (A) The Oxford thalamic connectivity atlas. (B-G) Comparison of the target thalamic subregion with other regions. *, P<0.05. ROI, region of interest; PD, Parkinson's disease; HC, healthy control.

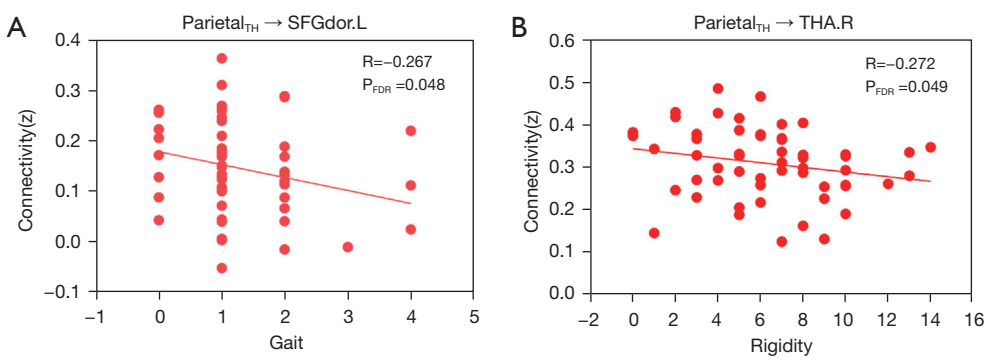

Figure 4 The significant results for relationships between thalamic functional connectivity and the clinical scores in the early-stage PD group after FDR correction. (A) The correlation of the functional connectivity between Parietal$_{TH}$ and SFGdor.L with gait score in the early-stage PD group. (B) The correlation of functional connectivity between the Parietal$_{TH}$ and THA.R with rigidity score in early-stage PD. Parietal$_{TH}$, parietal thalamus; SFGdor.L, left dorsolateral part of the superior frontal gyrus; THA.R, right thalamus; PD, Parkinson's disease; FDR, false discovery rate.

various thalamic subregions, including between the primary motor and sensory regions, sensory and occipital regions, and occipital and parietal regions. Finally, these alterations in functional connectivity pattern between the parietal thalamus and SFGdor.L and the right thalamus were related to motor signs in early-stage PD.

Thus far, the majority of studies in patients with PD have investigated the thalamus as a whole despite the differential connectivity and function of its subregions (25,26). In our study, we used ultrahigh-field imaging with voxel-based analysis to detect a pattern of reduced connectivity between five seeded thalamic subregions, including the primary motor thalamus, sensory thalamus, occipital thalamus, premotor thalamus, and posterior parietal thalamus, and relevant brain regions. The voxel-level analysis of thalamic subregions in previous 3-T MR studies has not been conducted to a sufficient extent (6,26). The sensitivity of BOLD fMRI is expected to increase super-linear enhancement with field strength (27), and a previous study indicated that ultrahigh-field 7-T BOLD fMRI may require a smaller sample size than may 3 T for exploring smaller regions within the thalamus (17). Therefore, we have good reason to believe that the results we detected are stable and reliable, as the sample in this study included 111 participants (55 in the PD group and 56 in the HC group).

In this study, we interestingly observed a pattern of reduced thalamic interconnectivity based on the ROI-wise level. No differences in thalamic interconnectivity were detected in the connectivity pattern between the thalamus and cortex at the voxel-level between the PD and HC groups. This discrepancy may be due to the different analytic approaches. The role of the thalamus and its subregions in PD have received considerable attention in clinical practice. A previous study suggested that levodopa could improve different the motor signs in PD through decreasing the functional connectivity of specific thalamic subregions (28). The functional connectivity patterns of thalamic subregions provide crucial information for distinguishing between patients with mild cognitive impairment and those with different motor subtypes of PD (6,7). However, the results of functional connectivity patterns noted in the abovementioned study differ from those in our study. These discrepancies may be due to several factors, including the variable impact on thalamic nuclei in the patients with PD, different combinations of PD, individual variations, and the use of different analytical methods. Nevertheless, the thalamic interconnectivity differences we detected using ultrahigh-field imaging provide additional data for clarifying the neural mechanisms of PD.

The thalamocortical connectivity reductions identified between PD and HC using voxel-based analysis prompted us to further explore their role in PD motor signs. Our observation that SFG was specifically affected in patients with PD with gait deficit is a new finding. Gait deficits are among the most debilitating signs of PD and often indicate that patients are at an increased risk of falls and have worsening disease severity (29). The relationship between the brain region in SFG and gait deficit could be interpreted as a reduction in the functional connectivity between the parietal thalamus and SFG being associated with higher gait scores. First, previous studies have demonstrated that the SFG plays an important role in the regulation of response inhibition (30,31). Specifically, the SFG has been shown to play a crucial role in the control of impulsive responses by regulating the inhibitory process (32). Considering these data together, we hypothesized that the decreased functional connectivity in SFG in patients with PD compared to HCs with higher gait scores may reflect the close relationship between dysfunction in the inhibitory control of the SFG and the severity of gait deficit. Second, another study demonstrated that SFG plays a crucial role in in integrating visual information with higher motor and cognitive functions (33). More recently, it was reported that severity of gait impairment and freezing was correlated with visual abnormalities (34). Thus, it has been proposed that a series of cortical connections from visual areas to motor areas underly the sensory guidance of movement (35). Therefore, we speculate that the SFG integrates visual information to guide gait control in patients with PD; however, this needs to be further confirmed with longitudinal data.

There are certain limitations to this study which should be acknowledged. One of the limitations is the use of Oxford thalamic connectivity atlas, as the use of other atlases might have led to different results. Although, the Oxford thalamic connectivity atlas is the primary atlas used in studies of thalamic subregions (17), examining other atlases is also essential. Another issue is the lack of longitudinal data. As we employed a case–control design, the functional changes identified in our study caused by the progression of disease should be further confirmed and longitudinal follow-up conducted in future research.

Conclusions

Through use of ultrahigh-field BOLD fMRI, we found a reduced functional connectivity pattern of the thalamocortical

circuit between the PD and HC groups. Additionally, the functional connectivity pattern between the parietal thalamus and SFGdor.L and the right thalamus in early-stage PD were related to gait and rigidity scores, respectively. Our results provide new insights into neural mechanisms underlying the pathophysiology of early-stage PD.

Acknowledgments

Funding: This research was supported by National Natural Science Foundation of China (Nos. 82151309 and 82327803 to X.L., and No. 82302146 to Y.X.).

Footnote

Reporting Checklist: The authors have completed the STROBE reporting checklist. Available at https://qims.amegroups.com/article/view/10.21037/qims-24-1498/rc

Conflicts of Interest: All authors have completed the ICMJE uniform disclosure form (available at https://qims.amegroups.com/article/view/10.21037/qims-24-1498/coif). The authors have no conflicts of interest to declare.

Ethical Statement: The authors are accountable for all aspects of the work in ensuring that questions related to the accuracy or integrity of any part of the work are appropriately investigated and resolved. This study was conducted in accordance with the Declaration of Helsinki (as revised in 2013) and was approved by the Chinese PLA General Hospital Ethics Committee (No. S2022-572-01). Informed consent was obtained from all individual participants.

References

1. Kalia LV, Lang AE. Parkinson's disease. Lancet 2015;386:896-912.
2. Lan Y, Liu X, Yin C, Lyu J, Xiaoxaio M, Cui Z, Li X, Lou X. Resting-state functional magnetic resonance imaging study comparing tremor-dominant and postural instability/gait difficulty subtypes of Parkinson's disease. Radiol Med 2023;128:1138-47.
3. Kwon DY, Kwon Y, Kim JW. Quantitative analysis of finger and forearm movements in patients with off state early stage Parkinson's disease and scans without evidence of dopaminergic deficit (SWEDD). Parkinsonism Relat Disord 2018;57:33-8.
4. Bloem BR, Okun MS, Klein C. Parkinson's disease. Lancet 2021;397:2284-303.
5. Zhang Y, Roy DS, Zhu Y, Chen Y, Aida T, Hou Y, Shen C, Lea NE, Schroeder ME, Skaggs KM, Sullivan HA, Fischer KB, Callaway EM, Wickersham IR, Dai J, Li XM, Lu Z, Feng G. Targeting thalamic circuits rescues motor and mood deficits in PD mice. Nature 2022;607:321-9.
6. Bu S, Pang H, Li X, Zhao M, Wang J, Liu Y, Yu H, Fan G. Structural and Functional Alterations of Motor-Thalamus in Different Motor Subtype of Parkinson's Disease: An Individual Study. Acad Radiol 2024;31:1605-14.
7. Li MG, He JF, Liu XY, Wang ZF, Lou X, Ma L. Structural and Functional Thalamic Changes in Parkinson's Disease With Mild Cognitive Impairment. J Magn Reson Imaging 2020;52:1207-15.
8. D'Cruz N, Vervoort G, Chalavi S, Dijkstra BW, Gilat M, Nieuwboer A. Thalamic morphology predicts the onset of freezing of gait in Parkinson's disease. NPJ Parkinsons Dis 2021;7:20.
9. Wang X, Xiong Y, Lin J, Lou X. Target Selection for Magnetic Resonance-Guided Focused Ultrasound in the Treatment of Parkinson's Disease. J Magn Reson Imaging 2022;56:35-44.
10. Xiong Y, Lin J, Pan L, Zong R, Bian X, Duan C, Zhang D, Lou X. Pretherapeutic functional connectivity of tractography-based targeting of the ventral intermediate nucleus for predicting tremor response in patients with Parkinson's disease after thalamotomy with MRI-guided focused ultrasound. J Neurosurg 2022;137:1135-44.
11. Cury RG, Fraix V, Castrioto A, Pérez Fernández MA, Krack P, Chabardes S, Seigneuret E, Alho EJL, Benabid AL, Moro E. Thalamic deep brain stimulation for tremor in Parkinson disease, essential tremor, and dystonia. Neurology 2017;89:1416-23.
12. Wang X, Wang S, Lin J, Zhang D, Lu H, Xiong Y, Deng L, Zhang D, Bian X, Zhou J, Pan L, Lou X. Gray matter alterations in tremor-dominant Parkinson's disease after MRgFUS thalamotomy are correlated with tremor

improvement: a pilot study. Quant Imaging Med Surg 2023;13:4415-28.
13. Xiong Y, Han D, He J, Zong R, Bian X, Duan C, Zhang D, Zhou X, Pan L, Lou X. Correlation of visual area with tremor improvement after MRgFUS thalamotomy in Parkinson's disease. J Neurosurg 2022;136:681-8.
14. Lin J, Kang X, Xiong Y, Zhang D, Zong R, Yu X, Pan L, Lou X. Convergent structural network and gene signatures for MRgFUS thalamotomy in patients with Parkinson's disease. Neuroimage 2021;243:118550.
15. Li Z, Lai Y, Li J, He N, Li D, Yan F, Zhang Y, Zhang C, Sun B, Wei H. BOLD frequency-dependent alterations in resting-state functional connectivity by pallidal deep brain stimulation in patients with Parkinson's disease. J Neurosurg 2023;139:1354-65.
16. Alper J, Seifert AC, Verma G, Huang KH, Jacob Y, Al Qadi A, Rutland JW, Patel S, Bederson J, Shrivastava RK, Delman BN, Balchandani P. Leveraging high-resolution 7-tesla MRI to derive quantitative metrics for the trigeminal nerve and subnuclei of limbic structures in trigeminal neuralgia. J Headache Pain 2021;22:112.
17. Hua J, Blair NIS, Paez A, Choe A, Barber AD, Brandt A, Lim IAL, Xu F, Kamath V, Pekar JJ, van Zijl PCM, Ross CA, Margolis RL. Altered functional connectivity between sub-regions in the thalamus and cortex in schizophrenia patients measured by resting state BOLD fMRI at 7T. Schizophr Res 2019;206:370-7.
18. Welton T, Hartono S, Shih YC, Schwarz ST, Xing Y, Tan EK, Auer DP, Harel N, Chan LL. Ultra-high-field 7T MRI in Parkinson's disease: ready for clinical use?-a narrative review. Quant Imaging Med Surg 2023;13:7607-20.
19. Cattarinussi G, Delvecchio G, Maggioni E, Bressi C, Brambilla P. Ultra-high field imaging in Major Depressive Disorder: a review of structural and functional studies. J Affect Disord 2021;290:65-73.
20. Postuma RB, Berg D, Stern M, Poewe W, Olanow CW, Oertel W, Obeso J, Marek K, Litvan I, Lang AE, Halliday G, Goetz CG, Gasser T, Dubois B, Chan P, Bloem BR, Adler CH, Deuschl G. MDS clinical diagnostic criteria for Parkinson's disease. Mov Disord 2015;30:1591-601.
21. Rajamani N, Friedrich H, Butenko K, Dembek T, Lange F, Navrátil P, et al. Deep brain stimulation of symptom-specific networks in Parkinson's disease. Nat Commun 2024;15:4662.
22. Hou Y, Luo C, Yang J, Ou R, Song W, Wei Q, Cao B, Zhao B, Wu Y, Shang HF, Gong Q. Prediction of individual clinical scores in patients with Parkinson's disease using resting-state functional magnetic resonance imaging. J Neurol Sci 2016;366:27-32.
23. Behrens TE, Johansen-Berg H, Woolrich MW, Smith SM, Wheeler-Kingshott CA, Boulby PA, Barker GJ, Sillery EL, Sheehan K, Ciccarelli O, Thompson AJ, Brady JM, Matthews PM. Non-invasive mapping of connections between human thalamus and cortex using diffusion imaging. Nat Neurosci 2003;6:750-7.
24. Tzourio-Mazoyer N, Landeau B, Papathanassiou D, Crivello F, Etard O, Delcroix N, Mazoyer B, Joliot M. Automated anatomical labeling of activations in SPM using a macroscopic anatomical parcellation of the MNI MRI single-subject brain. Neuroimage 2002;15:273-89.
25. Guan X, Zeng Q, Guo T, Wang J, Xuan M, Gu Q, Wang T, Huang P, Xu X, Zhang M. Disrupted Functional Connectivity of Basal Ganglia across Tremor-Dominant and Akinetic/Rigid-Dominant Parkinson's Disease. Front Aging Neurosci 2017;9:360.
26. Dirkx MF, den Ouden HE, Aarts E, Timmer MH, Bloem BR, Toni I, Helmich RC. Dopamine controls Parkinson's tremor by inhibiting the cerebellar thalamus. Brain 2017;140:721-34.
27. Uludağ K, Müller-Bierl B, Uğurbil K. An integrative model for neuronal activity-induced signal changes for gradient and spin echo functional imaging. Neuroimage 2009;48:150-65.
28. Liu W, Shen Y, Zhong Y, Sun Y, Yang J, Zhang W, Yan L, Liu W, Yu M. Levodopa improved different motor symptoms in patients with Parkinson's disease by reducing the functional connectivity of specific thalamic subregions. CNS Neurosci Ther 2024;30:e14354.
29. Kerr GK, Worringham CJ, Cole MH, Lacherez PF, Wood JM, Silburn PA. Predictors of future falls in Parkinson disease. Neurology 2010;75:116-24.
30. Dambacher F, Sack AT, Lobbestael J, Arntz A, Brugmann S, Schuhmann T. The role of right prefrontal and medial cortex in response inhibition: interfering with action restraint and action cancellation using transcranial magnetic brain stimulation. J Cogn Neurosci 2014;26:1775-84.
31. Chmielewski WX, Mückschel M, Dippel G, Beste C. Concurrent information affects response inhibition processes via the modulation of theta oscillations in cognitive control networks. Brain Struct Funct 2016;221:3949-61.
32. Zois E, Kiefer F, Lemenager T, Vollstädt-Klein S, Mann K, Fauth-Bühler M. Frontal cortex gray matter volume alterations in pathological gambling occur independently from substance use disorder. Addict Biol

2017;22:864-72.
33. Niu X, Gao X, Lv Q, Zhang M, Dang J, Sun J, Wang W, Wei Y, Cheng J, Han S, Zhang Y. Increased spontaneous activity of the superior frontal gyrus with reduced functional connectivity to visual attention areas and cerebellum in male smokers. Front Hum Neurosci 2023;17:1153976.
34. Uc EY, Rizzo M, Anderson SW, Qian S, Rodnitzky RL, Dawson JD. Visual dysfunction in Parkinson disease without dementia. Neurology 2005;65:1907-13.
35. Glickstein M. How are visual areas of the brain connected to motor areas for the sensory guidance of movement? Trends Neurosci 2000;23:613-7.

Cite this article as: Wang X, Xiong Y, Hu J, Li F, Duan C, Lu H, Zhang D, Huang J, Bian X, Wang S, Wang M, Yin X, Gao Z, Lou X. Thalamic functional connectivity on 7-Tesla magnetic resonance imaging and its relation to motor signs in early-stage Parkinson's disease. Quant Imaging Med Surg 2025;15(1):623-635. doi: 10.21037/qims-24-1498

